

Field induced spin transitions and large magnetoresistance in the quasi-one-dimensional magnet $\text{Ca}_3\text{Co}_2\text{O}_6$

Koji Yamada^{a,*}, Zentarou Honda^a, Jiaolian Luo^a, Hiroko Katori^b

^a Department Materials Science, Saitama University, Saitama 338-8570, Japan

^b Institute of Physical and Chemical Research, Wakoh, Saitama 351-0198, Japan

Received 6 September 2005; received in revised form 1 December 2005; accepted 5 December 2005

Available online 11 April 2006

Abstract

Magnetic and magnetoresistance effect of needle shaped crystal and slightly Co rich $\text{Ca}_3\text{Co}_2\text{O}_6$ was investigated in a temperature range between 2 and 100 K and in a dc magnetic field range less than 7 T and in pulsed fields less than 20 T. We found $1/3m_s$ and $2/3m_s$ plateaus of the magnetization for the full magnetization m_s and large negative magnetoresistance effect of 10% at the same magnetic fields, respectively.

Keywords: $\text{Ca}_3\text{Co}_2\text{O}_6$; Frustrated spin system; Quasi-one-dimensional magnet; Negative magnetoresistance

1. Introduction

The study of the magnetic properties of one-dimensional magnet has been a physical subject for a long time, particularly that exhibiting a spin transition to a three-dimensional long range ordered state caused by weak inter-chain interaction. The compound of $\text{Ca}_3\text{Co}_2\text{O}_6$ also belongs to these kinds of quasi-one-dimensional magnet showing a three-dimensional long range ordering state at low temperature.

$\text{Ca}_3\text{Co}_2\text{O}_6$ crystallizes in hexagonal lattice with space group $R\bar{3}c$ and lattice parameters $a = 907.93$ (7) pm and $c = 1038.1$ (1) pm at 298 K [1]. The crystal structure of $\text{Ca}_3\text{Co}_2\text{O}_6$ is shown in Fig. 1. $\text{Ca}_3\text{Co}_2\text{O}_6$ consists of infinite chains of alternating face sharing CoO_6 trigonal prisms and CoO_6 octahedra along the hexagonal c -axis. The inter-chain distance is 524 pm, which is about twice as large as the intra-chain Co distance of 259 pm. Each CoO_6 chains form a triangular network perpendicular to the c axis. Thus, we can expect exotic cooperative phenomena caused by the triangle lattice of the CoO_6 chains.

2. Sample preparation

Single phase powder samples of $\text{Ca}_3\text{Co}_2\text{O}_6$ and $(\text{Ca}_{1-x}\text{Sr}_x)_3\text{Co}_2\text{O}_6$ were synthesized as follows: mixtures

of CaCO_3 , SrCO_3 and CoO with the ratio $(\text{Ca}_{1-x}\text{Sr}_x):\text{Co} = 3:2$ were heated at 1173 K for 48 h in air. Single crystals of $\text{Ca}_3\text{Co}_2\text{O}_6$ and $(\text{Ca}_{1-x}\text{Sr}_x)_3\text{Co}_2\text{O}_6$ were grown by usual flux method (KCO_3 flux) as reported in Ref. [1]. Needle shaped crystals of several mm length were obtained.

3. Experimental results and discussion

The temperature dependence of the magnetic susceptibility of $\text{Ca}_3\text{Co}_2\text{O}_6$ has been measured. Below 24 K, a sudden increase of magnetic susceptibility is observed. Moreover, a second anomaly was observed at $T_{c2} = 12$ K which corresponds to the merging temperature of zero field cooling (ZFC) and field cooling (FC) magnetic susceptibility curves. Fig. 2 shows the temperature dependence of the magnetic susceptibility of Sr-doped $[\text{Ca}_{0.9}\text{Sr}_{0.1+x}]_3\text{Co}_2\text{O}_6$ single crystal. Here we aimed at a low sample resistance in a cryogenic temperature less than 24 K by doping Sr with small $x < 0.1$. A downward shift of T_{c2} is observed as Sr concentration increases. The downward shift of T_{c2} may be due to the changing of the inter-chain exchange interaction pathway by larger Sr ion doping. The magnetization processes up to 7 T are shown in Fig. 3. A linear increase in the magnetization versus magnetic field is observed at the paramagnetic range above T_{c1} ($T = 30$ K). In the temperature range of $T_{c1} > T > T_{c2}$, one can apparently see a plateau at one-third of the total magnetization ($1.3\mu_B/\text{f.u.}$). As seen in the magnetization process at $T = 2$ K, prominent magnetic hysteresis is observed. These results suggest that the spin (magnetic domain) freezing state appears below T_{c2} .

We performed the measurements of the sample resistance in zero field in a temperature range between 25 and 200 K. Fig. 4 shows the logarithmic plot of resistance as a function of the reciprocals of temperatures T . Here, we found the semiconductor nature of resistance change as a function of reciprocal temperatures for a Sr-doped extrinsic sample. Three activation energies were found at 50.4, 14.7 and 5.9 meV at respective temperature range as shown in the same figure under an assumption of activation type carriers. On the contrary, the hopping

* Corresponding author. Tel.: +81 48 858 3526; fax: +81 48 858 6465.

E-mail address: Yamasan@fms.saitama-u.ac.jp (K. Yamada).

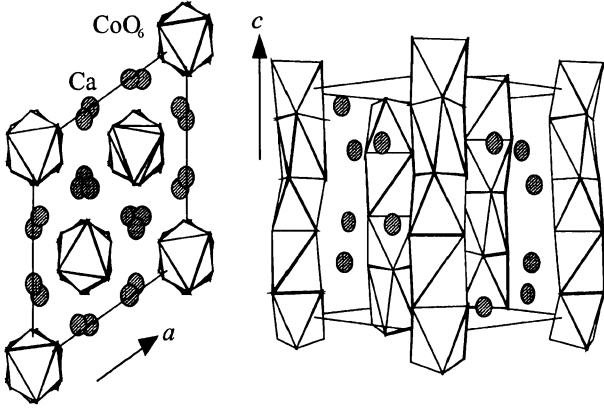


Fig. 1. Schematic view of the crystal structure of $\text{Ca}_3\text{Co}_2\text{O}_6$. (a) Projection (001); (b) CoO_6 chain structures.

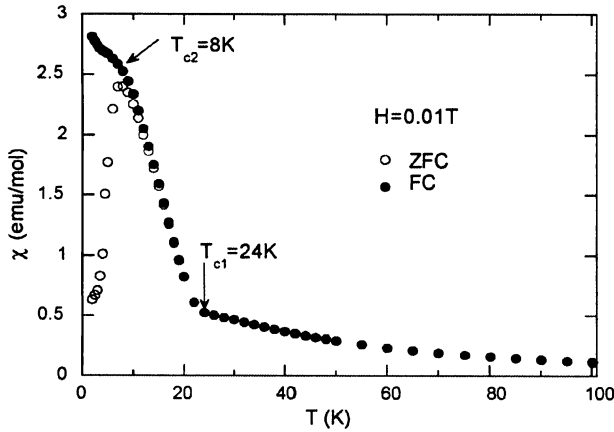


Fig. 2. Temperature dependence of the magnetic susceptibility of $(\text{Ca}_{0.9}\text{Sr}_{0.1})_3\text{Co}_2\text{O}_6$ ($H//c$ -axis). Note: the open symbols represent ZFC and closed circles FC.

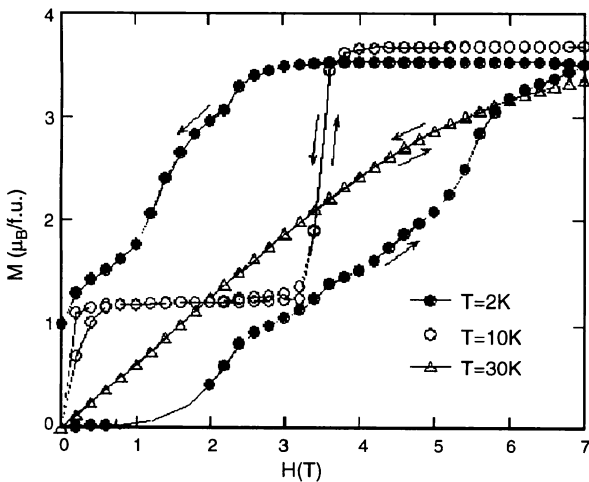


Fig. 3. Magnetization measurements in static magnetic fields up to 7 T for a $\text{Ca}_3\text{Co}_2\text{O}_6$ single crystal at several temperatures ($H//c$ -axis).

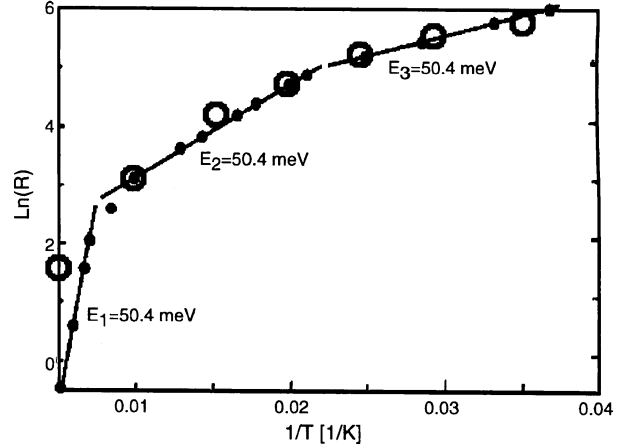


Fig. 4. Logarithmic plots of resistance change as a function of the reciprocal temperatures for the needle shaped sample.

conduction mechanism might be more plausible for this conductor. Therefore, by choosing the best fitting parameters for $c - \alpha(T)^{1/4}$ ($\alpha = 2.9$) logarithmic resistivity are plotted for comparison by large circles in Fig. 4 in a temperature range between 30 and 200 K.

The magnetoresistance (MR) effects of the same sample were also observed in pulsed magnetic fields up to 22 T together with the magnetization by using a pulsed magnet with 10 ms half-width. In these measurements, we adopted the method of noise eliminations as follows.

First, we observed the apparent sample drop voltages $V(I)$ given by the following equation as

$$V(I) = IR_s(B) + V_n(B), \quad (1)$$

Here, I stands for the current in the sample fed by the constant current source, $V_n(B)$, the inevitably included noise voltage caused by the pulsed high field, $R_s(B)$, the sample resistance as a function of magnetic field B , respectively. We also measured $V(-I)$ in the reversed sample current in the same pulsed field B at the same geometrical configuration, which generates the same noise voltage around the sample. By using the relation of Eq. (1), true sample drop voltage $V_s = IR_s(B)$ can be obtained [4] as

$$V_s = \frac{V(I) - V(-I)}{2} = IR_s(B). \quad (2)$$

The transient data of resistances and the magnetizations were recorded by using analogue to digital converter (ADC) with 16 bits resolution, $8\ \mu\text{s}/\text{words}$ and up to 16K words. The magnetization measurements in pulsed fields were performed by using a pick-up coil of flux change in a sample, composed of a triple-fold coil arranged along the main coil axis in the main solenoid coil. Here, the MR effect was simultaneously observed by using the method mentioned just above. As shown in Fig. 5 a little difference of the magnetization between that in dc field and that in transient pulsed fields was found in the low field range less than 9 T. These differences are plausibly understood by the temporal dispersion of the magnetization caused by the magnetic domain formations in the material. Note here that the notation "O" in Fig. 5 stands for the initial positions of the magnetization and MR, respectively at time $t=0$ for the field sweep. MR in this experiment could be understood by carrier density change and/or the mobility change with changing the magnetization, or with small change in the sample temperatures. Here, the behaviors of MR as a function of transient magnetizations as shown in Fig. 5 must be understood consistently. Here we plausibly adopt a physical model that the conductivity modification in a low field range less than 9 T as in Fig. 5, is caused by the mobility increase linearly with decreasing the carrier scatterings by the lattice site spin fluctuations. The maximum applied fields in the present MR experiment were limited below 9 T in a cryogenic temperature range to avoid the frequency dispersions of the magnetic system and to compare those magnetisms in dc fields as in Fig. 3. Here, the resistivity decreases with decreasing spin fluctuations of the lattice site spins for sample magnetizations. Now in a magnetization range between "O" and "A" (1.7 T) as

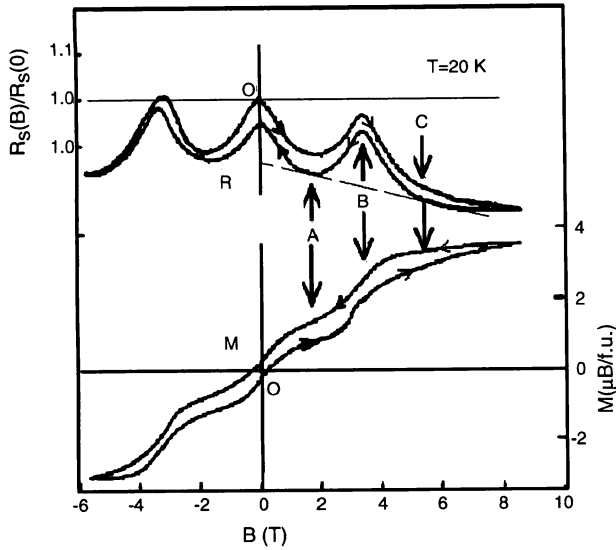


Fig. 5. Relative magnetoresistance and magnetization as a function of transient applied fields up to 9 T at $T=20$ K in the field configuration of $I//c//B$.

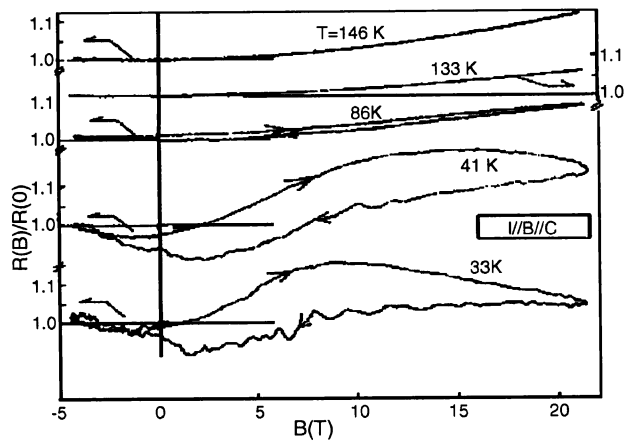


Fig. 6. MR in high pulsed fields higher than 22 T at different temperatures.

inserted in Fig. 5, where the spin fluctuations and the frustration ceased around at $M_S/3$ (M_S , the saturation magnetization). In contrast to this phenomena, in the magnetization range between "A" and "C", there must be the maximum spin fluctuations around at "B" (3.3 T) ($M=2M_S/3$) caused by the meta-magnetic phase transition between $(\uparrow\downarrow\downarrow)$ and $(\uparrow\uparrow\uparrow)$ spin configurations. In this study, we first report the maximum spin fluctuations observed via the resistance maximum in transient magnetizations. In the largest magnetization range around at "C" (5.2 T), almost all spins of carriers and lattice site spins are parallel due to the strong enough field reflected by the minimum resistivity. Here, it is also noticed that the after-effect of the magnetization in the pulsed fields, the background sample temperature must be slightly modified as seen in Fig. 5. It must be noted here that the experiment of MR was performed under pulsed fields with a short

half-width of 30 ms, which is not long enough to avoid the frequency dispersions of the magnetic system in this material. The hysteric nature and the temporal delay of the sample magnetization in the first rise pulsed fields up to 22 T as shown in Fig. 6, give rise to the hysteric resistance change and the time delay of the resistance change as a function of time elapses. Therefore, the responses of MR showed the different MR behaviors for the different increasing rates of the magnetic fields as that in Fig. 5 and those in Fig. 6 [2,3]. As shown in Fig. 6, we observed MR in a temperature range between 25 and 146 K, where the MR in a temperature range higher than 86 K, shows no hysteresis any more and always showed positive MR, reflected by the non-magnetic physical origin. In contrast to the slow rise field as that in Fig. 5, the negative MR caused by the spin scatterings of carriers played small role in the time duration of field increasing due to the insensitive magnetization even in the cryogenic temperature at 45 K. The hysteric MR traces in Fig. 6 in the cryogenic temperatures were totally caused by the temporal delay of the magnetizations and not caused by the technical faults of the MR measurements.

4. Conclusion

In this study, we found the peculiar behaviors of magnetization caused by the frustrated spin system with quasi-one-dimensional crystal structure of $\text{Ca}_3\text{Co}_2\text{O}_6$. Reflected by the spin fluctuations, MR showed the same magnetic field dependences except the positive MR at high temperature range. In addition to the hysteric nature, MR maximum was first found around at meta-magnetic phase transition in $T=20$ K between $(\uparrow\downarrow\downarrow)$ and $(\uparrow\uparrow\uparrow)$ spin configuration. The sample and the carrier in the present experiment, shows extrinsic nature and the MR in the cryogenic temperatures might be caused by the extrinsic carrier scatterings with spin system. For the future investigation of MR, the slow rise pulsed magnet longer than 30 ms half-width might be necessary to avoid the time delay of the slow-rise magnetization in this material. Further, the exact information on the magnetic structure in this material should be determined by the neutron scattering.

Acknowledgment

We would like to thank to Mr. Sugita for his devotion to make single crystals of $\text{Ca}_3\text{Co}_2\text{O}_6$ system with different dopant of Sr, etc.

References

- [1] H. Fjellvag, E. Guldbrandsen, S. Olsen, B.C. Hauback, J. Solid State Chem. 124 (1996) 190.
- [2] H. Kageyama, K. Yoshimura, K. Kosuge, M. Azuma, M. Takano, H. Mitamura, T. Goto, J. Phys. Soc. Jpn. 66 (1997) 3996.
- [3] A. Maignan, C. Michel, A.C. Masset, C. Martin, B. Raveau, Eur. Phys. J. B15 (2000) 657.
- [4] K. Yamada, J. Luo, Z. Honda, Proceedings of the Fifth Pan-pacific International Conference, Beijing, 2004, p. 2189.